Journal of Fluids and Structures (1999) **13,** 461–479
Article No.: jfls.1999.0215 available online at http://www.idealibrary.com on IDEAL

TRANSVERSE NATURAL FREQUENCIES AND FLOW-INDUCED VIBRATIONS OF DOUBLE BELLOWS EXPANSION JOINTS

V. JAKUBAUSKAS AND D. S. WEAVER

Department of Mechanical Engineering, McMaster University
Hamilton, Ont., Canada L8S 4L7

(Received 25 November 1998 and in revised form 26 February 1999)

This paper considers the transverse vibrations of fluid-filled double-bellows expansion joints. The bellows are modelled as a Timoshenko beam, and the fluid added mass includes rotary inertia and bellows convolution distortion effects. The natural frequencies are given in terms of a Rayleigh quotient, and both lateral and rocking modes of the pipe connecting the bellows units are considered. The theoretical predictions for the first six modes are compared with experiments in still air and water and the agreement is found to be very good. The flow-induced vibrations of the double bellows are then studied with the bellows downstream of a straight section of pipe and a 90° elbow. Strouhal numbers are computed for each of the flow-excited mode resonances. The bellows natural frequencies are not affected by the flowing fluid but the presence of an immediate upstream elbow substantially reduces the flow velocity required to excite resonance.

1. INTRODUCTION

BELLOWS EXPANSION JOINTS are corrugated pipes which have been used to absorb axial, transverse and rotational movement in piping systems for more than 100 years. In recent years, this technology is replacing expansion loops in power plant piping because it is much more compact and reduces head loss. It has also found significant applications in the aerospace industry. In cases where the pipe lateral movement is large, double bellows, as shown in Figure 1(a), may be used. Since these joints are quite flexible, lateral supports may be utilized to prevent buckling, [Figure 1(b)].

The flexibility of bellows makes them susceptible to flow-induced vibration. Above some critical velocity, the bellows develop large-amplitude oscillations at one of the bellows natural frequencies, and fatigue failures occur in a relatively short time. In order to predict the limiting flow velocity for a bellows, it is necessary to have an accurate estimate of the bellows natural frequencies.

The early studies on bellows vibrations concentrated on axial vibrations and provided relatively simple formulae for frequency predictions (Gerlach 1969; EJMA 1980). Weaver & Ainsworth (1989) conducted an experimental study of a double bellows which had experienced service failure, and suggested that the self-excitation of bellows was associated with shear layer instability across the cavities of the individual bellows convolutions and occurred for a constant Strouhal number of 0·45. This was confirmed using data from other bellows (Weaver 1989) and by a scaled-up, two-dimensional laboratory model (Gidi & Weaver 1995). A more recent study by Jakubauskas & Weaver (1996) found that the bellows axial stiffness predictions of Gerlach (1969) and EJMA (1980) could be in error, as

0889–9746/99/040461 + 19 $30.00

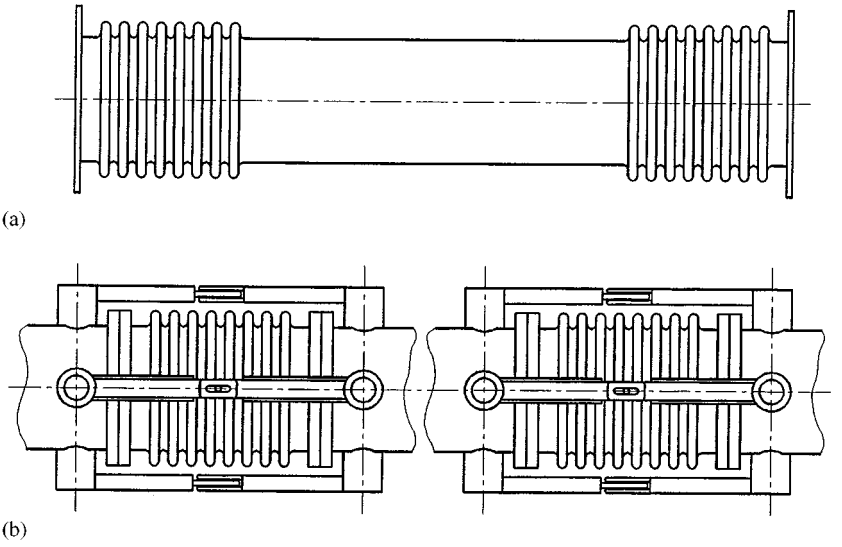

Figure 1. (a) Double bellows; (b) double bellows with lateral supports.

could be the fluid added mass predictions, although the latter could compensate for the former error in certain cases of bellows containing liquids.

Li *et al.* (1986) studied transverse vibrations of a single bellows using a simple Bernoulli–Euler beam solution, as does the EJMA Standard (1980). Morishita *et al.* (1989) used a Timoshenko beam model and claimed that, while shear can be ignored, the effect of rotary inertia of bellows was significant. This was verified in the studies of Jakubauskas & Weaver (1998a, b), who also showed that convolution shape distortion produces a component of added mass which is dominant in vibration modes higher than the first, especially for shorter bellows. For the single bellows studied, these authors demonstrated that the neglect of rotary inertia and convolution distortion in the EJMA Standard produced significant over-predictions of even the first mode of transverse vibration. No similar study appears in the technical literature for double bellows.

This paper presents an analysis of the transverse vibration of double-bellows expansion joints. The analysis models a bellows as a Timoshenko beam containing a flowing fluid and neglecting the effect of transverse shear. The results are presented in the form of a Rayleigh quotient to facilitate hand calculation. The natural frequency predictions are verified in air and quiescent fluid. Flow-induced vibration experiments in a water tunnel are also presented for cases when the bellows have a straight pipe and an elbow directly upstream of the bellows.

2. THEORETICAL ANALYSIS

The theoretical analysis follows directly the approach taken by Jakubauskas & Weaver (1998a,b), and the only details important to the present study will be presented here. The second of these papers (1998b) showed that the bellows could be modelled as a Timoshenko beam neglecting shear. Furthermore, it was shown that the Coriolis and curvature effects of the flowing fluid could be ignored for the flow velocities used in practical applications of bellows. Thus, the equation of motion for transverse vibration of bellows with flowing fluid

is given by

$$EI_{eq}\frac{\partial^4 w}{\partial x^4} + m_{tot}\frac{\partial^2 w}{\mathrm{d}t^2} - \rho I\frac{\partial^4 w}{\partial x^2 \partial t^2} + P\pi R_{\mathrm{m}}^2\frac{\partial^2 w}{\partial x^2} = 0, \tag{1}$$

where EI_{eq} is the bellows equivalent bending stiffness per unit length, m_{tot} is the total mass of the bellows per unit length including fluid added mass, ρI is the effective mass moment of inertia (rotary inertia of the bellows and contained fluid), P is the internal pressure, R_m is the mean radius of the bellows (see Figure 2), w is the lateral bellows displacement, and x is the axial coordinate. Jakubauskas & Weaver (1998b) developed analytical expressions for each of the parameters in equation (1) in terms of the bellows geometry and material properties.

The equivalent bending stiffness of the bellows, EI_{eq}, is written in terms of the bellows axial stiffness, k, the bellows convolution pitch, p, and the bellows mean radius, R_m, as follows:

$$EI_{eq} = \tfrac{1}{4}\,kpR_m^2. \tag{2}$$

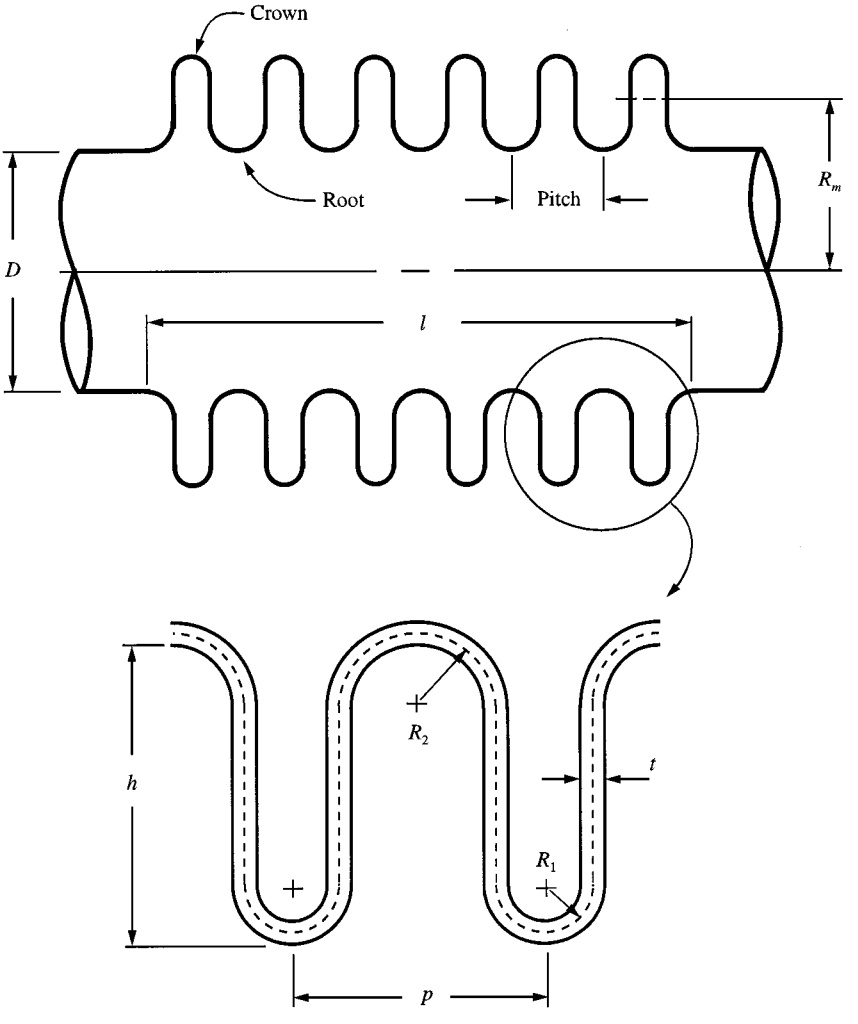

Figure 2. Bellows geometry.

It should be noted that the relatively simple expressions for axial stiffness given by Gerlach (1969) and EJMA (1980) may be somewhat in error (Jakubauskas and Weaver 1996). For this reason, Gerlach recommended using measured axial stiffness for improved frequency predictions. For calculations in the present paper, the authors have used the axial stiffness computed from their finite-element shell model which has been demonstrated to provide excellent results (Jakubauskas and Weaver 1996).

The rotary inertia of the bellows is given by

$$\rho I = \pi R_{\mathrm{m}}^3 \left[\left(\frac{2h}{p} + 0{\cdot}571 \right) t p_b + \frac{h}{p} (2R_2 - t) \rho_f \right], \tag{3}$$

where h is the convolution height, t is the convolution material thickness, and ρ_b and ρ_f are the densities of the bellows material and fluid, respectively. The first term in equation (3) is the rotary inertia of the bellows, while the second term is that of the fluid trapped between the convolutions.

The total mass per unit length of the bellows, m_{tot}, is comprised of three components: that due to the bellows itself, that due to the rigid-body motion of the fluid contained in the bellows, and that due to the shape distortion of the bellows convolutions (fluid added mass due to radial acceleration of the fluid squeezed in and out of the convolutions during vibration); i.e.,

$$m_{tot} = \frac{4\pi R_m}{p} (h + 0{\cdot}285p) t \rho_b + \left[\pi \left(R_m - \frac{h}{2} + \frac{2hR_2}{p} \right)^2 + \alpha_{f2k} \mu R_m^3 \right] \rho_f, \tag{4}$$

where μ is the fluid added mass coefficient and α_{f2k} is the coefficient

$$\alpha_{f2k} = 0{\cdot}066 \frac{A_{lk}^2}{l^4} \left(R_m - \frac{h}{2} \right)^2 p. \tag{5}$$

In equation (5), l is the bellows length and A_{lk} is a function of the normalized mode shape of the kth mode, X_k,

$$A_{lk} = \left[\frac{\int_0^1 X_k''(\xi)^2 \, \mathrm{d}\xi}{\int_0^1 X_k(\xi)^2 \, \mathrm{d}\xi} \right]^{1/2}. \tag{6}$$

The primes in equation (6) represent differentiation with respect to the normalized axial coordinate ξ, i.e. $x/l = \xi$.

The fluid added mass coefficient, μ, was found by Jakubauskas & Weaver (1998a) using a finite-element model of the fluid contained by the bellows during vibration, and the results for typical bellows geometries are plotted in Figure A1. Thus, knowing the bellows and fluid densities, the bellows geometry as shown in Figure 2, and the fluid added mass coefficient from Figure A1, all the parameters in the equation of motion, equation (1), can be determined. It remains to solve this equation subject to the appropriate boundary conditions.

2.1. Boundary Conditions

Double bellows generally consist of two identical single bellows units at either end of a relatively rigid connecting pipe, as shown in Figure 1(a). Since double bellows are symmetric about their centreline, it is only necessary to consider half the double bellows for lateral

vibration analysis, as shown in Figure 3. The bellows unit has a total length of l and the half-length of the connecting pipe is a. Figure 3(a) shows the first lateral mode of vibration, in which the motion of the connecting pipe is pure translation. This is true of all lateral modes, the second and third of which are shown in Figure 3(b, c). Figure 4(a) shows the first rocking mode, in which the connecting pipe rotates about its centre. This is true for all rocking modes, the second and third of which are shown in Figure 4(b, c). These two mode types are treated separately, because of the different boundary conditions created by these distinct motions. For generality, a lateral support stiffness, k_s, and the support effective mass, M_s, have been placed at the right end of the bellows, as shown in Figures 3(a) and 4(a).

The left-hand side of the bellows in Figures 3 and 4 is fixed through a flange to a pipe which is rigid compared to the bellows. Therefore, the lateral displacement and rotation at this flange are zero:

$$w(0, t) = \frac{\partial w}{\partial x}(0, t) = 0. \tag{7}$$

2.1.1. *Lateral modes* (*pure translation of connecting pipe*)

For lateral modes, the rotation of the right end of the bellows is also zero, i.e.

$$\frac{\partial w}{\partial x}(l, t) = 0. \tag{8}$$

The fourth boundary condition arises from the requirement that the shear force at the right end of the bellows is equal to the combined inertia force of lateral support mass, M_s, and the mass of the half connecting pipe and contained fluid, $(m_p + m_f)a$, and the force of the lateral support stiffness, $k_s w$; i.e.,

$$\frac{\partial^3 w(l,\ t)}{\partial x^3} = \frac{1}{EI_{eq}}\left\{[M_s + (m_p + m_f)a]\frac{\partial^2 w(l, t)}{\partial t^2} + k_s \mathrm{w}(l, \mathrm{t})\right\}, \tag{9}$$

where m_p and m_f are the mass per unit length of the connecting pipe and contained fluid, respectively.

2.1.2. *Rocking modes* (*pure rotation of connecting pipe about its centre*)

The geometric boundary condition at the right end of the bellows during rocking modes arises from the fact that the slope is known from the simple rotation angle, θ, of the connecting pipe about its centreline,

$$\theta = -\frac{\partial w(l, t)}{\partial x} = \frac{w(l, t)}{a}. \tag{10}$$

The fourth boundary condition is rather more complex but again is derived from the shear force at the right end of the bellows. The equation of motion of the half connecting pipe about its pivot is given by

$$J_p \frac{\partial^2 \theta}{\partial t^2} = M(l, t) + Q(l, t)a - k_s w(l, t)a, \tag{11}$$

where J_p is the moment of inertia of the half connecting pipe including contained fluid and support mass about the pivot, and $M(l, t)$ and $Q(l, t)$ are the moment and shear force, respectively, produced by the bellows acting on the end of the connecting pipe. The final

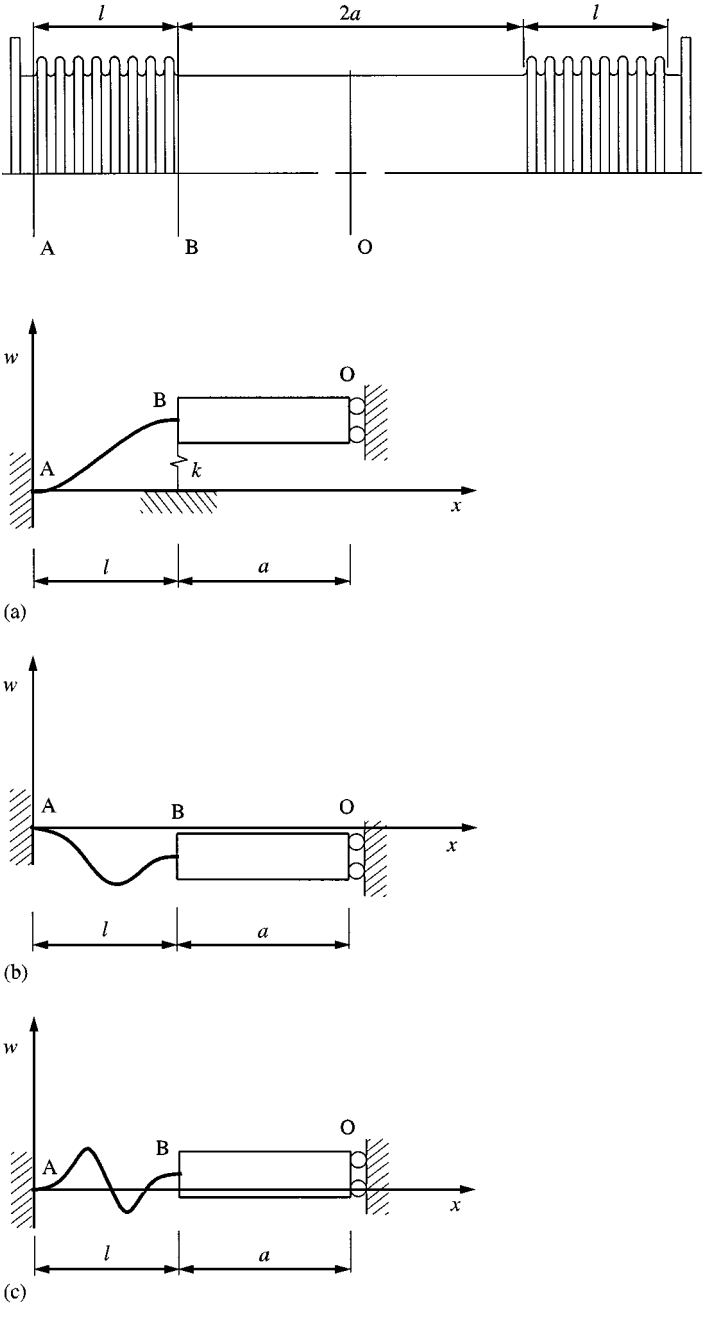

Figure 3. Double bellows section. (a) First lateral mode; (b) second lateral mode; (c) third lateral mode.

term on the right-hand side of equation (11) is the moment created by the lateral support stiffness, k_s. Considering now the equilibrium of an element of the bellows with internal pressure, P, the shear force, Q, is given by

$$Q = \frac{\partial M}{\partial x} + P\pi R_m^2 \frac{\partial w}{\partial x} - \rho I \frac{\partial^3 w}{\partial x \partial t^2}, \tag{12}$$

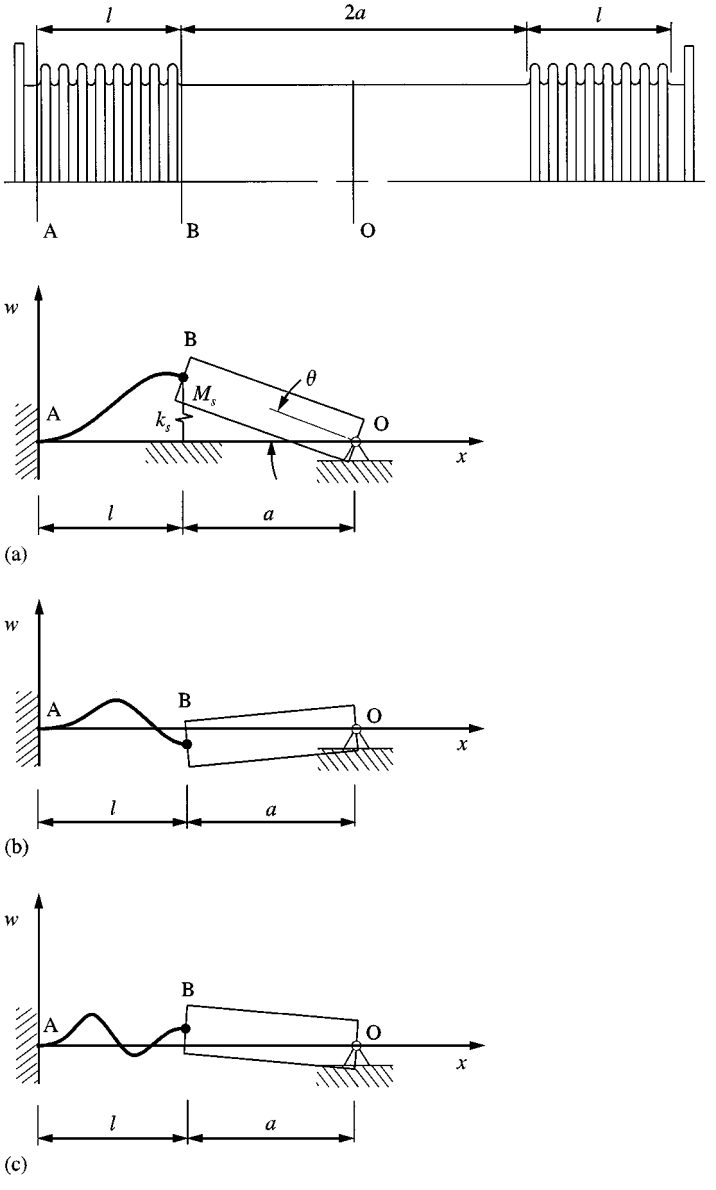

Figure 4. Double bellows section. (a) First rocking mode; (b) second rocking mode; (c) third rocking mode.

where the third term on the right-hand side represents the rotary inertia of the bellows and contained fluid, and shear effects in the Timoshenko beam theory have been neglected as discussed in the foregoing. This expression was used to derive the general equation of motion, equation (1), [see, for example, Païdoussis & Li (1993), Blevins (1990), and Timoshenko *et al.* (1974)].

Using the moment curvature relationship for the bellows,

$$M = EI_{eq}\frac{\partial^2 w}{\partial x^2}, \tag{13}$$

and the geometric relationship for the half connecting pipe,

$$\frac{\partial^2\theta}{\partial t^2} = \frac{1}{a}\frac{\partial^2 w}{\partial t^2} \tag{14}$$

with equations (11) and (12) at the bellows boundary, $x = l$, provides the final boundary condition:

$$\frac{\partial^3 w(l,t)}{\partial x^3} = -\frac{1}{a}\frac{\partial^2 w(l,t)}{\partial x^2} + \frac{1}{EI_{eq}}\left[k_s w(l,t) \quad - P\pi R_m^2 \frac{\partial w(l,t)}{\partial x} + \rho I \frac{\partial^3 w}{\partial x \partial t^2} + \frac{J_p}{a^2}\frac{\partial^2 w(l,t)}{\partial t^2}\right]. \tag{15}$$

The moment of inertia of the connecting pipe about the pivot including support mass, M_s, and contained fluid is given by

$$J_p = \frac{(m_p + m_f)a^3}{3} + \frac{(2m_p + m_f)aR^2}{4} + M_s a^2, \tag{16}$$

where R is the mean radius of the connecting pipe. In equation (16), the half pipe has been modelled as a thin-walled circular cylinder of radius R and length a, and the fluid has been modelled as a solid cylinder of the same dimensions. For moments of inertia of such sections, see for example Blevins (1979).

3. SOLUTION OF EQUATION OF MOTION

The solution procedure follows that outlined in Jakubauskas & Weaver (1998b). Assuming a solution in the form

$$w(x, t) = X(x)\sin \omega t \tag{17}$$

and substituting into the equation of motion, equation (1), yields an ordinary differential equation in the axial coordinate, x. Then following the Rayleigh quotient approach, this equation is multiplied by the mode shape function of the *kth* mode, X_k, which satisfies all of the appropriate boundary conditions for the case considered. After integrating by parts, the frequency equation for the kth natural frequency becomes

$$f_k = \frac{R_m}{4\pi l^2} A_{lk}\left[\frac{kp - 4\pi l^2 P A_{2k} + (4k_s l^3 A_{3k}/R_m^2}{m_{tot} + (\rho I A_{4k})/l^2 + B A_{5k}}\right]^{1/2}, \tag{18}$$

where

$$B = [M_s + (m_p + m_f)a]/l \quad \text{for lateral modes}$$

$$B = \frac{J_p}{a^2 l} \quad \text{for rocking modes} \tag{19}$$

and the A_{ik} are functions of the mode shapes:

$$A_{2k} = \frac{\int_0^1 (X_k')^2 \,\mathrm{d}\xi}{\int_0^1 (X_k'')^2 \,\mathrm{d}\xi}, \quad A_{3k} = \frac{X_k^2(1)}{\int_0^1 (X_k'')^2 \,\mathrm{d}\xi}, \quad A_{4k} = \frac{\int_0^1 (X_k')^2 \,\mathrm{d}\xi}{\int_0^1 X_k^2 \,\mathrm{d}\xi}, \quad A_{5k} = \frac{X_k^2(1)}{\int_0^1 X_k^2 \,\mathrm{d}\xi}, \tag{20}$$

and A_{lk} was defined in equation (6). It should be noted that the mode shape functions in equation (20) have been written in terms of the dimensionless coordinate, $\xi = x/l$, i.e. $X(\xi)$. When the mode shape functions satisfying the appropriate boundary conditions are known, the constants A_{ik} can be determined once and for all.

TABLE 1

A_{ik} constants for lateral modes

Mode no.	No lateral Supports			Lateral supports
A_{ik}	1	2	3	1
A_{1k}	5·650	Figure A2	Figure A3	5·62
A_{2k}	0·10	0·0249	0·0119	0·0998
A_{3k}	0	0	0	0·0826
A_{4k}	3·193	Figure A2	Figure A3	3·152
A_{5k}	2·656	Figure A2	Figure A3	2·611

TABLE 2

A_{ik} Constants for rocking modes

Mode no.	No Lateral Supports			Lateral Supports
A_{ik}	1	2	3	1
A_{1k}	Figure A4	Figure A5	Figure A6	Figure A7
A_{2k}	Figure A4	Figure A5	Figure A6	Figure A7
A_{3k}	0	0	0	Figure A7
A_{4k}	3·08	Figure A5	Figure A6	3·073
A_{5k}	Figure A4	Figure A5	Figure A6	Figure A7

The constants A_{ik} were computed using the mode shapes derived from the Bernoulli–Euler equation. In some cases, it was found that these constants were essentially independent of the length of the connecting pipe, $2a$. In other cases, the constants were found to depend on a and were plotted as functions of a/l, as shown in Figures A2–A7, for the first three natural frequencies of both lateral and rocking modes. The results are summarized in Tables 1 and 2 for lateral and rocking modes, respectively. Also provided in these tables are the constants for the first modes of double bellows with lateral supports.

The above analysis was developed so that the natural frequencies of double bellows could be computed using hand calculations. To check the accuracy of the approximate Rayleigh quotient approach, the solutions for the first mode of vibration were obtained from an exact solution of the differential equation of motion and appropriate boundary conditions. For both the first lateral and rocking modes, the Rayleigh quotient approach was less than 1% off the exact solution. This is not unexpected as it is well known that a good approximation for the assumed mode functions in the Rayleigh quotient produces an even better approximation of the natural frequencies, and the assumed mode shapes used to compute the constants of equation (20) are expected to be very good (eigenfunctions of the Bernoulli–Euler equation satisfying the correct boundary conditions).

4. EXPERIMENTAL VERIFICATION

A special rig was designed to determine the natural frequencies of the bellows with static air and water inside. The fixture was capable of being pressurized and was made sufficiently rigid so that its lowest natural frequency was an order of magnitude above the bellows

natural frequencies of interest. Vibrations were monitored using strain gauges carefully placed on the bellows convolutions, such that axial and bending modes could be separated. Details of the test fixture and strain gauge arrangement are given in Jakubauskas & Weaver (1998b).

The natural frequencies were obtained by shock excitation of the bellows and analysing the strain gauge signals with a Fourier Analyzer in its transient capture mode. The bellows used in the experiments were made from stainless steel with the following parameters: $R_m = 0{\cdot}0844$ m, $h = 0{\cdot}0158$ m, $R_1 = 0{\cdot}00308$ m, $R_2 = 0{\cdot}00268$ m, $l = 0{\cdot}1517$ m, $t = 0{\cdot}0006$ m, $a = 0{\cdot}1502$ m, $p = 0{\cdot}01152$ m, $p_b = 7860$ kg/m, $E = 2{\cdot}07 \times 10^{11}$ Pa, $k = 3{\cdot}7 \times 10^6$ N/m, and $v = 0{\cdot}3$.

The experimental results are summarized in Table 3 and compared with theoretical predictions for internal air at $P = 0$ and 200 kPa and water at $P = 0$. It is seen that the predictions for the natural frequencies in air with zero internal gauge pressure are quite good, with a maximum error for the first six modes (three lateral and three rocking) of less than 4%. The agreement with internal air pressurized to 200 kPa is nearly as good, with a maximum error of less than 5%. It is important to note that the effect of internal pressure is to lower the natural frequencies. This effect is greatest for the first lateral mode (about 8%) and essentially disappears by the third lateral or rocking mode. The predictions for natural frequencies in water with zero gauge pressure are also in reasonable agreement with experiments, with the errors being less than 5% except for the third lateral mode (7·5%). Interestingly, the predictions for the rocking modes are generally better than those for the lateral modes for the bellows used in these tests. The authors have no explanation for this and cannot judge whether this would be expected for other double bellows. However, it is considered that the agreement of the predictions with experiments is good for all the modes studied. Experiments were also conducted for internal water pressurized to 200 kPa (Jakubauskas 1995). The effect of internal pressure on natural frequency was less for water than for air and the agreement of theory with experiment was similar to that shown in Table 3, so the detailed results are not presented here.

Calculations were also conducted for the first lateral and rocking mode frequencies of these bellows in air and water at zero gauge pressure using Bernoulli-Euler beam theory and the formulae of EJMA (1980), as shown in Table 4. The results show that the neglect of rotary inertia by Bernoulli–Euler theory leads to an error of the order of 20% for the first lateral and rocking modes in air. This effect is expected to increase with higher mode numbers. Interestingly, the effect of rotary inertia seems to be less significant for natural frequency predictions for double bellows in water, presumably because added mass effects are dominant. Similar results were observed for single bellows, although in that case the

TABLE 3

Summary of experimental results (Exp) and comparison with theoretical predictions (Theo)

	Air ($P = 0$)			Air ($P = 200$ kPa)			Water ($P = 0$)		
Mode	Exp(Hz)	Theo(Hz)	%Error	Exp(Hz)	Theo(Hz)	%Error	Exp(Hz)	Theo(Hz)	%Error
Lat_1	78·8	81·2	3·0	72·5	75·5	4·1	35·0	36·0	2·9
Roc_1	119	121	1·7	111	116	4·5	61·0	62·3	2·1
Lat_2	284	294	3·5	278	289	4·0	186	194	4·3
Roc_2	305	311	2·0	296	306	3·4	206	208	1·0
Lat_3	458	475	3·7	456	471	3·3	319	343	7·5
Roc_3	482	488	1·2	480	484	0·8	338	352	4·1

TABLE 4

Comparison of present theory with Bernoulli–Euler and EJMA (1980)

Mode	Air ($P = 0$)			Water ($P = 0$)		
	Experiment	Bernoulli-Euler	EJMA	Experiment	Bernoulli-Euler	EJMA
Lat_1	78·8	91·8	91·8	35	37·2	51·0
Roc_1	119	143	158	61	66·0	89·1

differences were much greater (Jakubauskas and Weaver 1998b). Table 4 also shows that the predictions of EJMA are generally rather poor, with frequency estimates ranging from 17 to 46% high. This is apparently due to the neglect of rotary inertia and errors in estimating the axial stiffness and fluid added mass of the bellows.

5. FLOW-INDUCED VIBRATION EXPERIMENTS

Since the motivation for this work was to obtain the natural frequencies of bellows for determining the limiting velocities for flow-induced vibration, the bellows used in the above tests were placed in a water tunnel for experiments with internal flow. The double bellows were placed in a straight section of pipe for uniform flow and then placed immediately downstream of a standard 90° elbow to determine the effect of nonuniform flow. Details of the water tunnel and test procedure are given in Jakubauskas & Weaver (1998b) for the case of a single-bellows unit.

The test results are plotted as vibration r.m.s. amplitude response against mean flow velocity in Figures 5 and 6 for the cases of a straight pipe upstream and an elbow upstream of the bellows, respectively. The amplitude response is shown on an arbitrary scale since it is the output of strain gauges on one of the bellows convolutions. Thus, bending strain is being measured and, since the bending of that convolution depends on the mode, this strain cannot be interpreted directly as a vibration amplitude.

The response curves of Figures 5 and 6 are qualitatively similar to those reported by Weaver & Ainsworth (1989) and Jakubauskas & Weaver (1998b) for a relatively small double and a single bellows, respectively. No significant response is observed until the flow velocity reaches some critical value, then a succession of vibration modes are excited as the flow velocity is increased further. The vibration amplitudes of the bellows convolutions were sufficiently large that they could be seen visually and were accompanied by an audible humming sound. The first mode observed was the second axial mode at 136 Hz, in which the connecting pipe is stationary with the bellows at each end oscillating out-of-phase with one another. This was also the first mode observed in the experiments of Weaver & Ainsworth (1989) with a much smaller double bellows. Apparently, the damping in the first axial mode (53 Hz) is sufficiently high to overcome the excitation energy available at the critical velocity for that mode. It seems that this is also true for the lowest lateral and rocking modes which would be expected at 35 and 61 Hz, respectively. The initial lateral and rocking modes to be excited were the second modes at 186 and 206 Hz, respectively. Note that the second lateral mode was only observed when the bellows was placed downstream of the elbow. The next peak observed at 264 Hz is the fourth axial mode, there being no evidence of the third axial mode at 167 Hz. Finally, the third lateral and rocking modes were observed. The experiment was stopped at a flow velocity of about 9 m/s.

Several important observations can be made from Figures 5 and 6. Firstly, as noted above, the first mode to be excited is not necessarily the lowest natural frequency. At present

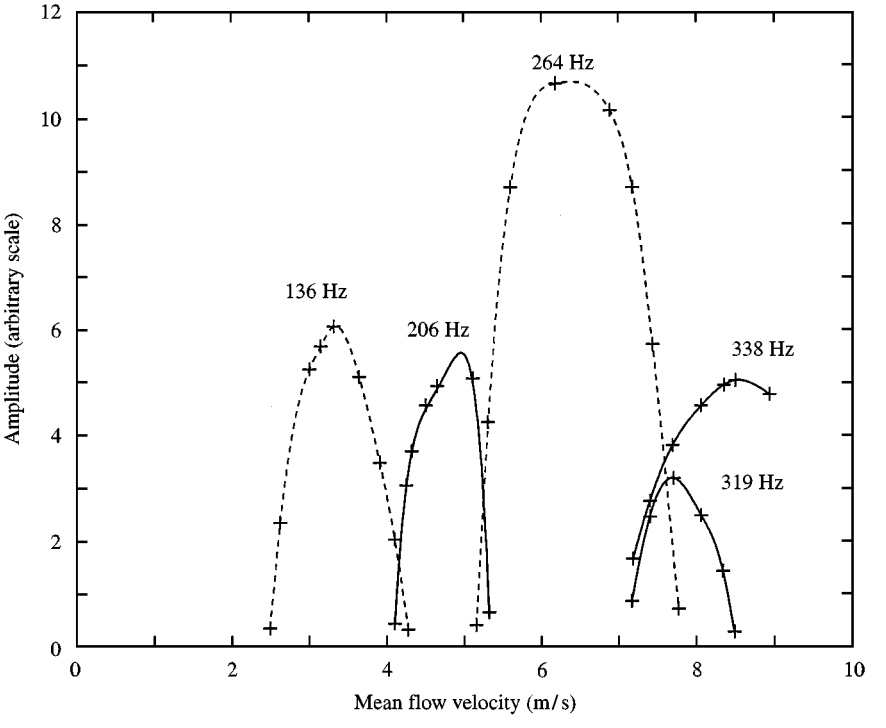

Figure 5. Bellows response with straight pipe upstream.

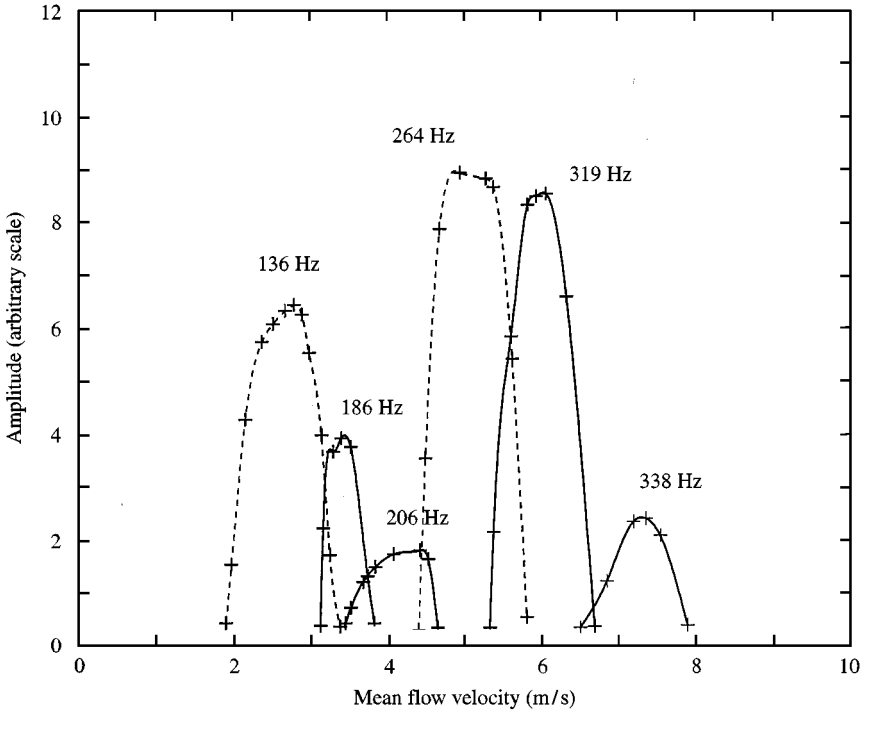

Figure 6. Bellows response with elbow upstream.

TABLE 5

Summary of Strouhal numbers

Mode	2nd Axial	Lat_2	Roc_2	4th axial	Lat_3	Roc_3
Frequency (Hz)	136	186	206	264	319	338
Strouhal Numbers						
Away from elbow	0·46	–	0·46	0·44	0·47	0·46
At elbow	0·56	0·63	0·54	0·60	0·61	0·53

there exists no method to account for the effect of damping on critical mode excitation. It should be noted that the lowest natural frequency (first axial mode) was critical with the single bellows studied by Jakubauskas & Weaver (1998b). Secondly, the frequencies excited by the flow are identical to those observed in quiescent fluid which means that the flow has no obvious effect on the bellows natural frequencies. Finally, the effect of an upstream elbow is to significantly reduce the mean flow velocity at which flow excitation occurs. This means that a high velocity flow over only a portion of the circumference of the bellows convolutions is sufficient to cause large-amplitude flow-induced vibration.

The Strouhal number, St, for bellows is based on mean flow velocity, V, measured at the peak response amplitude, the frequency of vibration, f, and the convolution pitch, p, as the length scale:

$$\mathrm{St} = \frac{fp}{V}. \tag{21}$$

Strouhal numbers for the response peaks in Figures 5 and 6 were computed and are summarized in Table 5. The average Strouhal number for the response peaks of the bellows away from an upstream elbow is 0·46 with a standard deviation of 0·01. This agrees well with the value of 0·45 reported by Weaver & Ainsworth (1998b) for a small double bellows and by Jakubauskas & Weaver (1998b) for a single bellows. The Strouhal number for the bellows just downstream of the 90° elbow has an average value of 0·58 with a standard deviation of 0·04. This means that placing the bellows near an elbow has reduced the limiting velocity for flow excitation by more than 20%.

6. CONCLUSIONS

A theoretical model has been developed for computing the natural frequencies of transverse vibrations of double bellows expansion joints. The theory is based on Timoshenko beam theory, neglecting the effects of shear but including fluid added mass and rotary inertia. The model treats lateral and rocking modes separately and is presented in the form of a Rayleigh quotient. The model predictions are compared with experimental results in air and both quiescent and flowing water. Comparison is also made with the predictions of Bernoulli–Euler beam theory and the EJMA Standard (1980). The conclusions are as follows.

1. The agreement between the present theory and experiment is reasonable, with errors in the first three lateral and rocking modes in both air and water generally being less than 5%.

2. The effect of internal pressurization is to reduce the natural frequencies but, practically speaking, this effect is not large and diminishes with increasing mode number.

3. The effect of rotary inertia, which is neglected in both the Bernoulli–Euler and EJMA approaches, is significant, especially for vibrations in air.

4. The EJMA predictions significantly overestimate the transverse natural frequencies of the bellows tested, because rotary inertia is neglected and the simple estimates for stiffness and added mass are not sufficiently accurate, at least for the bellows tested in this study.

5. Internal flow has a negligible effect in the natural frequencies of bellows.

6. The mean flow velocity at the flow-induced vibration response peaks of double bellows can be reasonably estimated using the convolution pitch as the length scale with a Strouhal number of 0·45. This is the same value as found for axial vibrations of single bellows.

7. The effect of an elbow directly upstream of a bellows is to significantly reduce the mean flow velocity required to produce large amplitude flow induced vibrations.

ACKNOWLEDGEMENTS

The authors gratefully acknowledge the financial support of the Natural Sciences and Engineering Research Council of Canada.

References

Blevins, R. D. 1979 *Formulas for Natural Frequency and Mode Shape*. New York: Van Nostrand Reinhold.

Ejma 1980 *Standards of the Expansion Joint Manufacturers Association Inc*., 5th edition. New York: EJMA.

Gerlach, C. R. 1969 Flow-induced vibrations for metal bellows. *ASME Journal of Engineering for Industry* **91,** 1196–1202.

Gidi, A. & Weaver, D. S. 1995 A model study of flow induced bellows vibration. *Proceedings of 6th International Conference on Flow Induced Vibration* (ed. P. Bearman), pp. 497–503. Rotterdam: A.A. Balkema.

Jakubauskas, V. F. 1996 Transverse vibrations of bellows expansion joints. Ph.D. Thesis, McMaster University, Hamilton, Canada.

Jakubauskas, V. F. & Weaver, D. S. 1996 Natural vibration of fluid filled bellows. *ASME Journal of Pressure Vessel Technology* **118,** 484–490.

Jakubauskas V. F. & Weaver, D. S. 1998a Transverse vibrations of bellows expansion joints. Part I: Fluid added mass. *Journal of Fluids and Structures* **12,** 445-456.

Jakubauskas V. F. & Weaver, D. S. 1998b Transverse vibrations of bellows expansion joints, Part II: Beam model development and experimental verification. *Journal of Fluids and Structures* **12,** 457–474.

Li, T. X., Li, T. X. & Guo, B. L. 1986 Research on axial and lateral natural frequencies of bellows with different end conditions. Paper 86-PVP-14. New York: ASME.

Morishita, M., Ikahata, N., & Kitamura, S. 1989 Dynamic analysis methods of bellows including fluid-structure interaction. In *Metallic Bellows and Expansion Joints*-1989 (eds C. Becht IV, A. Imazu, R. Jetter & W.S. Reimus), PVP-Vol. 168, pp. 149-157. New York: ASME.

Weaver, D. S. 1989 Flow induced vibrations and stability of bellows. *Proceedings of 1st International Conference on Engineering Aero-Hydroelasticity* (*EAHE*). Vol. 1, pp. 37–46. Prague, Czechoslovakia.

Weaver, D. S. & Ainsworth, P. 1989 Flow induced vibrations in bellows. *ASME Journal of Pressure Vessel Technology* **111** 402–406.

APPENDIX 1: ADDED MASS AND MODE COEFFICIENTS

In this appendix typical plots of added mass coefficients and mode coefficients are presented for a typical range of bellows parameters.

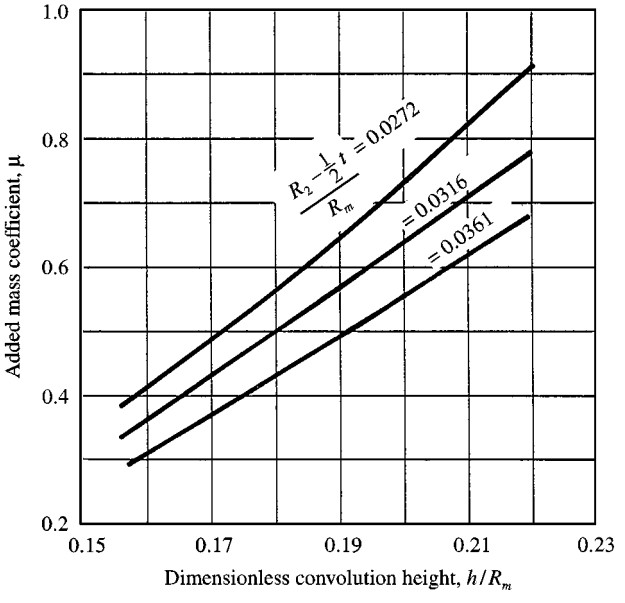

Figure A1. Fluid added mass coefficient, from Jakubauskas & Weaver (1998a).

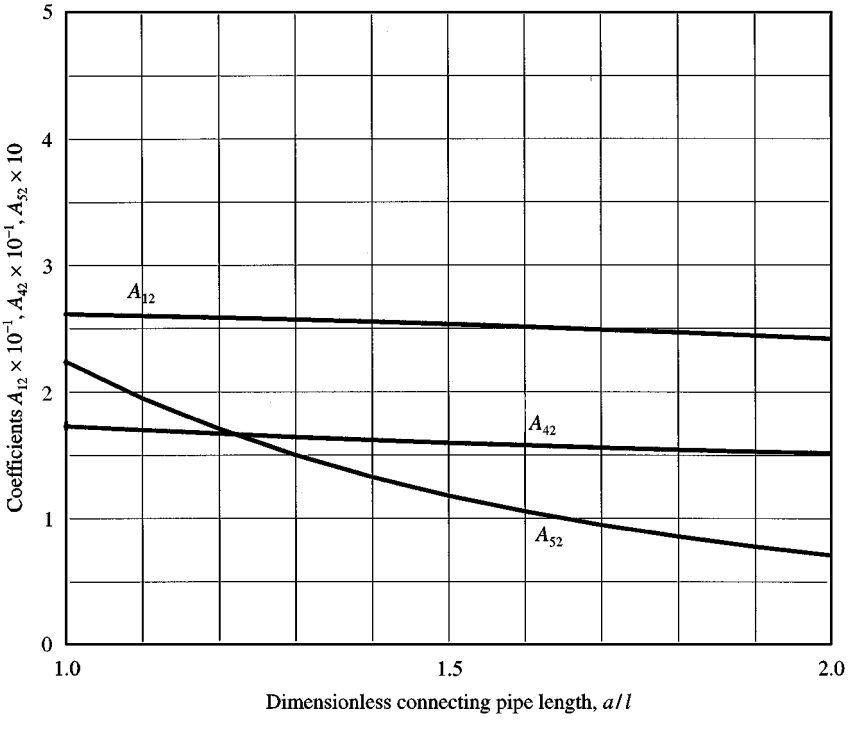

Figure A2. Coefficients for second lateral mode, no lateral support.

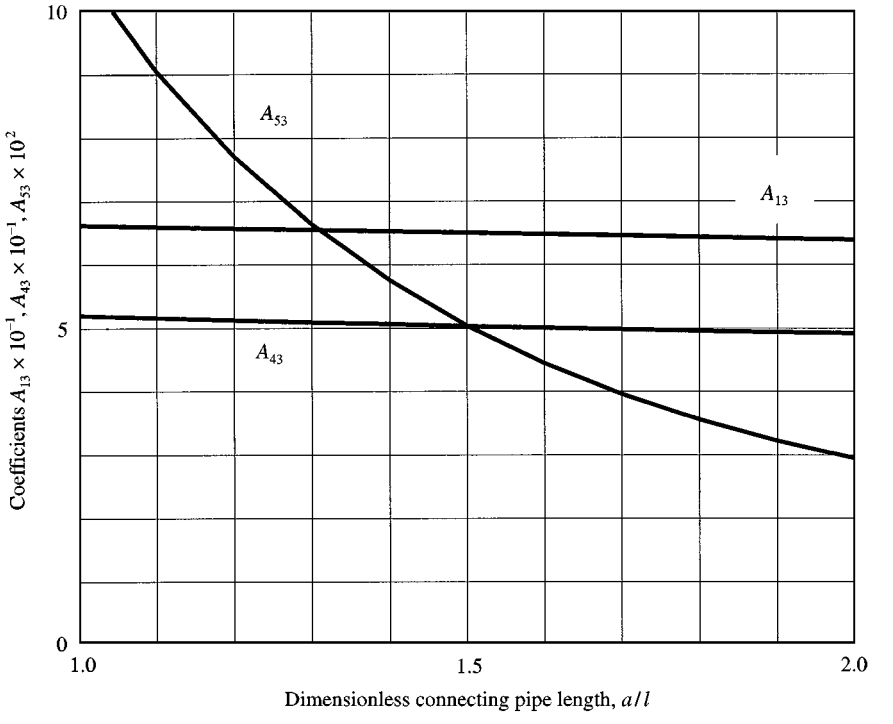

Figure A3. Coefficients for third lateral mode, no lateral support.

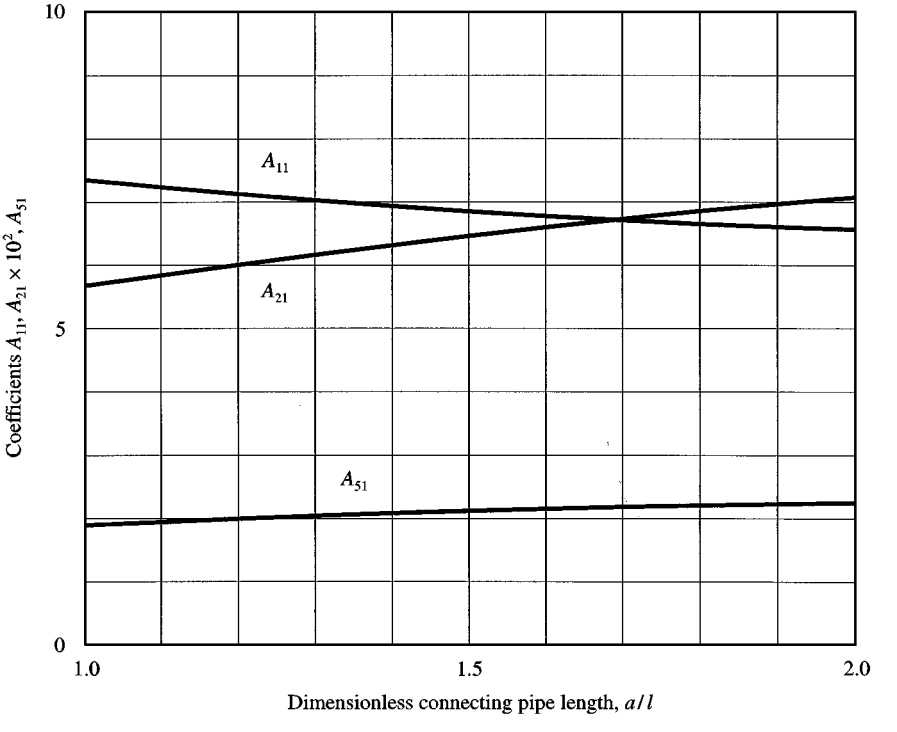

Figure A4. Coefficients for first rocking mode, no lateral support.

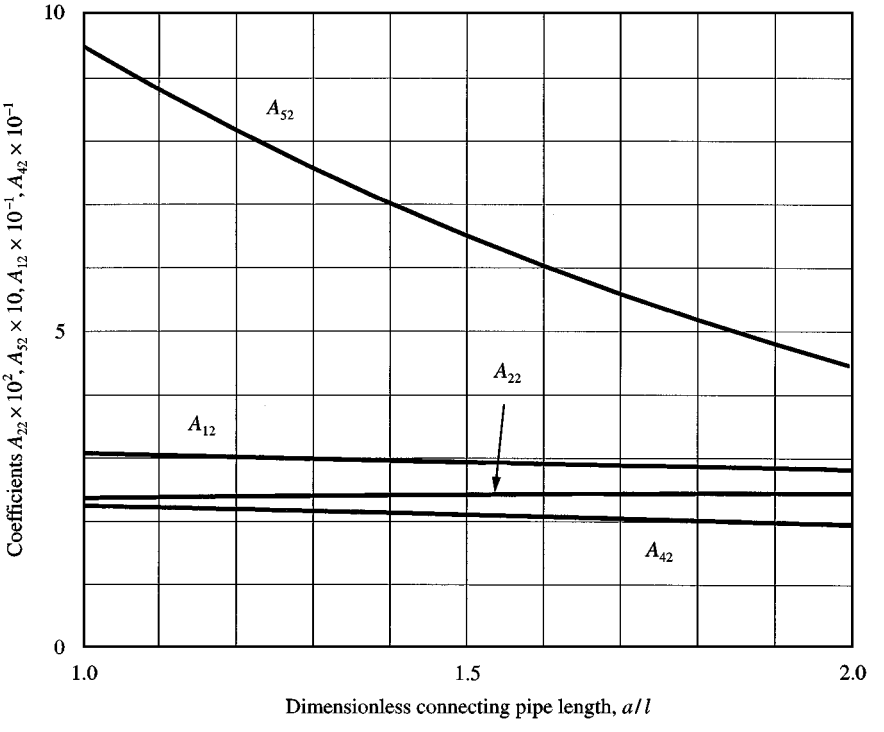

Figure A5. Coefficients for second rocking mode, no lateral support.

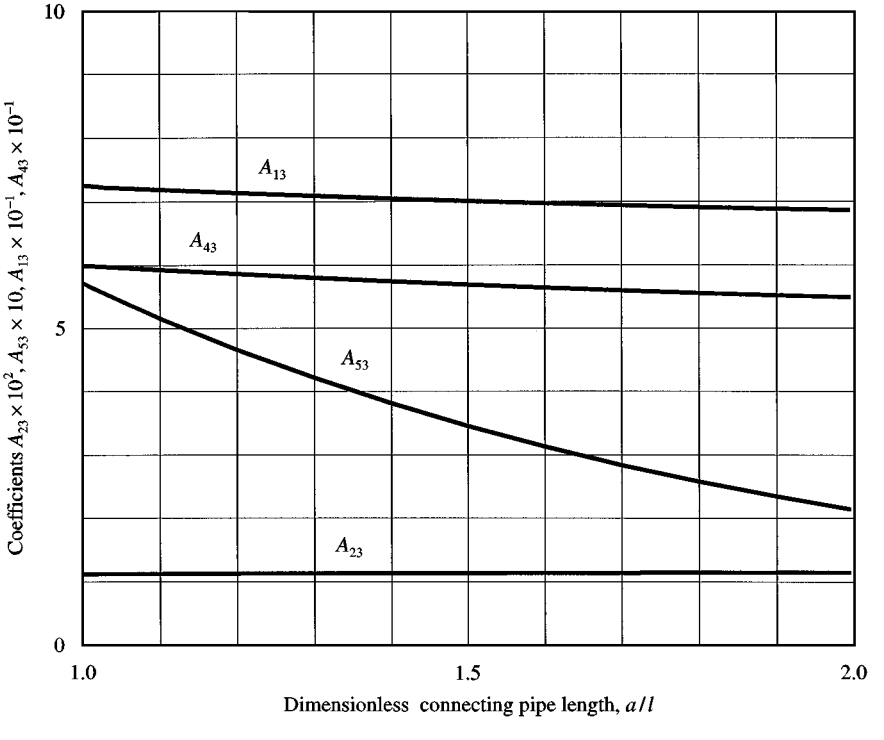

Figure A6. Coefficients for third rocking mode, no lateral support.

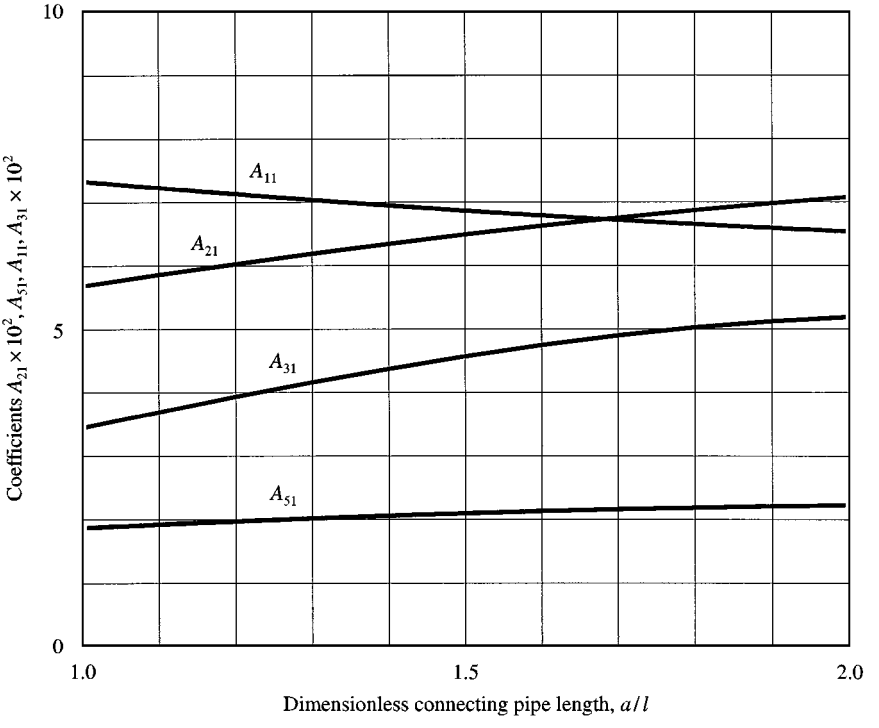

Figure A7. Coefficients for first rocking mode with lateral support.

APPENDIX 2: NOMENCLATURE

A_{ik}	ith constant for mode k
a	half-length of connecting pipe
B	constant
E	modulus of elasticity
EI_{eq}	equivalent bending stiffness of bellows
f	frequency at resonance peak
f_k	frequency in kth mode (Hz)
h	total convolution height
J_p	mass moment of inertia of half-connecting pipe about pivot
k	axial stiffness of bellows per half-convolution
k_s	lateral support stiffness
l	live length of bellows
M	bending moment
M_s	lateral support effective mass
m_{tot}	total bellows mass per unit length (including fluid added mass)
m_b	bellows mass per unit length
m_p	connecting pipe mass per unit length
p	convolution pitch
P	fluid pressure
Q	shear force
R	mean radius of connecting pipe
R_1	convolution root radius
R_2	convolution crown radius
R_m	mean radius of bellows
St	Strouhal number
t	bellows convolution thickness and time

V	mean flow velocity through bellows
w	transverse displacement
X_k	bellows mode shape in kth mode
x	axial coordinate
α_{f2k}	integral function for bellows distortion fluid added mass in kth mode
θ	rotation angle of connecting pipe about pivot
μ	added mass coefficient
ρ	density
ρ_b	density of bellows material
ρ_f	fluid density
ρI	effective mass moment of inertia (rotary inertia) of bellows and contained fluid
ω	frequency (rad/s)

Subscript

k	kth mode